

УДК 539.1.074.55

STUDY OF THE SILICON DRIFT DETECTOR PERFORMANCE WITH INCLINED TRACKS

S. Kouchpil^{a,b}, *D. Nouais*^c, *E. Crescio*^c, *M. Bondila*^{d,g},
P. Cerello^c, *P. Giubellino*^c, *L. Montano*^{c,e}, *S. Piano*^f,
C. Piemonte^f, *A. Rashevsky*^f, *L. Riccati*^c, *A. Rivetti*^c,
F. Tosello^c, *W. H. Trzaska*^d, *A. Vacchi*^f, *R. Wheadon*^c

^a Joint Institute for Nuclear Research, Dubna

^b NPI, Řež, Czech Republic

^c INFN Sezione di Torino, Italy

^d HIP, Jyväskylä University, Finland

^e CINVESTAV Mexico City

^f INFN Sezione di Trieste, Italy

^g Institute of Space Sciences, Bucharest

The position resolution of a full-size prototype silicon drift detector designed for the ALICE experiment was measured as a function of incident angle by using a pion beam of 140 GeV/c at the CERN SPS, and the results are presented in this paper. The anodic resolution is seen to improve significantly as the angle increases, as expected. The dependences of cluster charge and cluster size on incident angle are also reported.

Измерено пространственное разрешение как функция угла наклона кремниевого дрейфового детектора — прототипа, созданного для эксперимента ALICE. Проанализированы экспериментальные данные, полученные при облучении детектора пионами с импульсом 140 ГэВ/с на SPS в ЦЕРН. Как и ожидалось, разрешение вдоль направления анодов детектора значительно улучшается с увеличением наклона трека. Приводятся зависимости суммарного заряда кластера и размера кластера от угла наклона трека.

INTRODUCTION

The Silicon Drift Detectors (SDD) [1] will equip the third and the fourth layers of the ALICE Inner Tracking System (ITS) [2]. A detailed description of the ALICE SDD can be found in [3]. Several prototypes have been tested using beam particles. An overview of the results of these studies can be found in [4–9].

This article presents the study of the influence of the incident particle angle with respect to the detector on the performance of the ALICE SDD. The motivations of this study, as well as the expected behavior of the SDD performance with nonperpendicular incident tracks are described in Sec. 1. The experimental conditions are described in Sec. 2, and the results are presented and discussed in Sec. 3.

1. MOTIVATIONS AND EXPECTED BEHAVIOR

1.1. Motivations. The ALICE-ITS consists of six coaxial silicon detector layers with the z axis coinciding with the beam direction [2]. Layer 3 (15 cm radius) consists of 14 ladders each supporting six SDDs, and layer 4 (24 cm radius) consists of 22 ladders each supporting eight SDDs.

Let $\theta_{r\phi}$ be the angle between the direction perpendicular to the detector plane and the track projection on the $r\phi$ plane (Fig. 1, *a*).

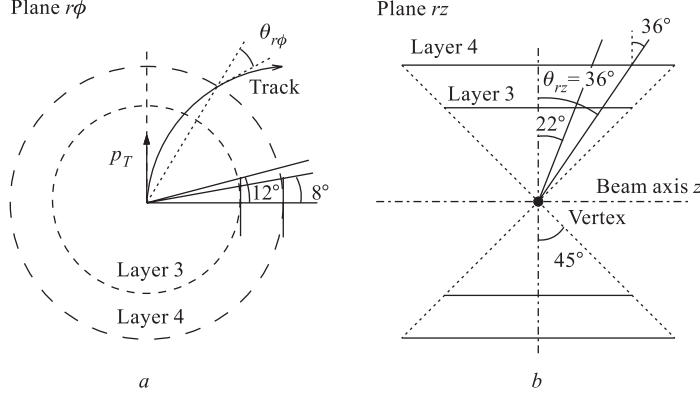


Fig. 1. Schematic view of the SDD layers of the ITS. In the $r\phi$ plane (*a*), the incident angle of the tracks on the detectors depends on the particle transverse momentum and the impact point on the detector. In the rz plane (*b*) the incident angle depends essentially on the particle scattering angle

For high-momentum particles (or in absence of magnetic field), $\theta_{r\phi}$ ranges from 0 to 12° for layer 3 and from 0 to 8° for layer 4. The thickness of the SDD is $300 \mu\text{m}$. In the worst case of $\theta_{r\phi} = 12^\circ$, the inclination contributes to a spread of the electron cloud of about $\sigma_\theta = 300 \sin 12^\circ / \sqrt{12} = 18 \mu\text{m}$ r.m.s. This value is negligible compared to the cluster size after a drift time of $O(100 \text{ ns})$ because of the expansion due to the diffusion effect [8]. In the presence of the magnetic field, the angle $\theta_{r\phi}$ is modified by a value of $\delta\theta_{r\phi}$ depending on the transverse momentum p_T of the particle. The curves $\delta\theta_{r\phi}$ vs. p_T are represented in Fig. 2 for the nominal value of the magnetic field in ALICE $B = 0.5 \text{ T}$. Neglecting the interaction in the material, the minimum transverse momentum (threshold) that a particle needs to reach the outermost layer of the ITS is $p_T \simeq 64.5 \text{ MeV}/c$. The incident angle variation $\delta\theta_{r\phi}$ does not exceed 16° and decreases quickly as a function of p_T . The spatial resolution of the detector is not a critical issue in the

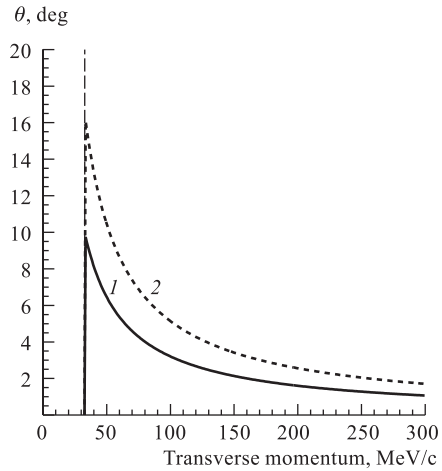


Fig. 2. Dependence of the angle of the incident particle on transverse momentum: 1 — inner SDD layer; 2 — outer SDD layer

tracking of low-momentum particles because of the dominant effect of the multiple scattering. For higher momentum the inclination of the track due to the magnetic field is negligible. Because of these considerations, a study of tracks inclined along the drift axis has not been carried out.

In the rz plane (Fig. 1, *b*), the angle θ_{rz} between the direction perpendicular to the detector and the track projection ranges from 0 to approximately 45° . The distribution of electrons released in the detector by an inclined track has rectangular shape of width $w \tan \theta_{rz}$ along the z axis, $w = 300 \mu\text{m}$ being the thickness of the detector.

Due to the diffusion effect, the electron distribution has a shape which is the convolution of the rectangular distribution and a Gaussian with a standard deviation $\sigma(t)$ typically within the range $30 \div 180 \mu\text{m}$ in the drift time interval $0 \div 5 \mu\text{s}$. Hence, the r.m.s. of the electron distribution in the anode direction as a function of the drift time is

$$\text{r.m.s.}(t) = \sqrt{\sigma^2(t) + \left(\frac{w \tan \theta_{rz}}{\sqrt{12}}\right)^2}. \quad (1)$$

Since the charge is collected by up to three SDD anodes only, the width and shape variations may have an important influence on the anodic spatial resolution.

In order to study the behavior of the SDD performance versus θ_{rz} , besides the standard set of data with perpendicular tracks, two sets of data have been taken with nonperpendicular tracks: $\theta_{rz} = 22.5^\circ$ and $\theta_{rz} = 36^\circ$.

1.2. Expected Behavior. As illustrated in Fig. 3, a charged particle crossing the detector at angle θ_{rz} passes a distance $w / \cos \theta_{rz}$ inside the detector that is larger than the thickness w of

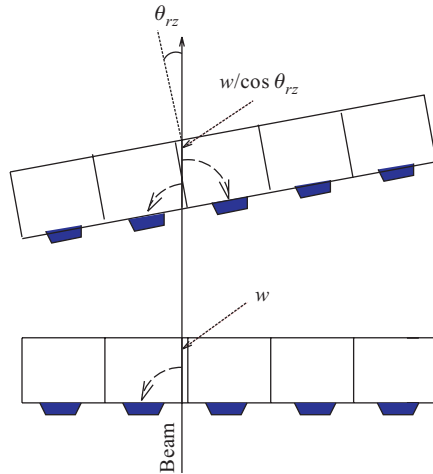


Fig. 3. Scheme of charge collected by two anodes with inclined tracks (top) and by a single anode in the detector with perpendicular tracks (bottom)

the wafer. Therefore, as an immediate consequence, the collected charge should increase by a factor $1 / \cos \theta_{rz}$ with respect to that released by a particle incident perpendicularly increasing the signal-to-noise ratio by 8% at 22.5° and by 24% at 36° . Moreover, the charge is expected to be shared, on average, by more adjacent anodes for any given drift time. The fraction of wider clusters should increase, while that of single anode clusters should decrease. Therefore an improvement of the anodic resolution is expected, especially in the part of the detector close to anodes where, in the case of perpendicular tracks, the high fraction of narrow clusters is responsible for the deterioration of the resolution. From geometrical considerations, the drift axis cluster size is not expected to change significantly. A small improvement of the spatial resolution along the drift direction is expected from the higher value of the signal-to-noise ratio (S/N) due to the inclination of the detector with respect to the beam axis. However, AliRoot simulations [10] have shown that a negligible influence is expected by increasing the S/N ratio by 20%. The drift axis resolution will not be studied in this paper.

2. EXPERIMENTAL DETAILS

2.1. Detector. All the studies were carried out with the ALICE SDD D2 prototype [3] (very close to the final design for ALICE) produced by Canberra Semiconductors N.V., Belgium. Each SDD is produced from a 300- μm -thick, 5-inch-diameter n -type silicon wafer of resistivity 3 $\text{k}\Omega \cdot \text{cm}$. The detector has a bi-directional structure with two opposite drift directions. For each drift region 292 p^+ cathodes are implanted on both sides of the wafer with 120- μm pitch. A voltage divider, implanted in the wafer, connects all the adjacent cathode strips with 170- $\text{k}\Omega$ resistors. For each half of the detector the drift length is 35.0 mm, and the drifting charge is collected by 256 anodes with a pitch of 294 μm , so that the sensitive area is 70 \times 75 mm. The active area of the SDD is 85% of its total area.

2.2. Experimental Setup. The experimental results presented in Sec. 3 were obtained from the analysis of the data taken at the CERN SPS with a pion beam at $p = 140$ GeV/c in August 2000. Figure 4 shows a scheme of the setup. To avoid multiple tracks, caused by event pile-up, a beam with a low intensity of 10^4 pions/burst was used. The nominal SDD drift field (667 V/cm) was used for the present study. The SDD was placed on the beam trajectory between two microstrip telescopes which measured the particle impact point on the SDD with a precision of ~ 5 μm r.m.s. Each of the microstrip detectors had an area of about 20 \times 20 mm and 50 μm pitch between strips. Two pairs of scintillating counters placed at the both ends of the setup provided the beam trigger signal. The microstrip telescopes were aligned with these trigger counters. The overlapping region between each pair of scintillators covered the same area as the microstrip planes. Since the SDD area was larger than the beam spot and the microstrip detectors sensitive area, the SDD was mounted on a micrometric XY -table with remote control system. The signals induced on the SDD anodes were amplified using OLA chips [11], specially developed for this type of detector, and sampled at 40 MHz by nonlinear 8-bit Flash ADCs. A relevant linearization procedure was applied to the data during the offline analysis. A complete description of the electronics chain and data acquisition system is given in [4].

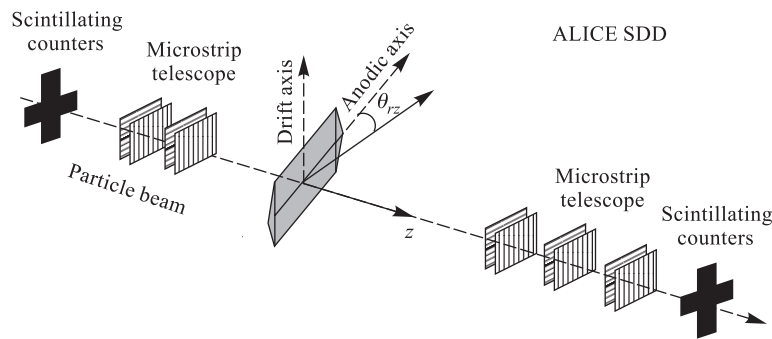


Fig. 4. Scheme of the beam test setup

2.3. Data. The data taking was organized in *runs*, in which a certain number of events (typically from 20 000 to 50 000) in the same experimental conditions, i.e., the SDD position, connected anodes, etc., were recorded. All runs were taken at the nominal drift field, with

single tracks. Runs Nos.4862–4872 and Nos.4891–4898 were performed with the detector support structure rotated at 22.5 and 36° with respect to the beam direction, respectively. The ranges of connected anodes for these two sets of data were different in order to avoid the presence of material from the mechanical support on the beam line. To compare the SDD performance for the same group of anodes, two sets of runs Nos.4737–4752 and Nos.4789–4805 taken with perpendicular tracks were used for the analysis. A summary of the data used for this analysis is shown in table.

Data used for the present analysis

	Runs	SDD anodes	Number of events
Perpendicular tracks, 0°	4789–4805	0–60	536 500
Inclined tracks, 22.5°	4862–4872	0–60	377 000
Perpendicular tracks, 0°	4737–4752	55–110	516 600
Inclined tracks, 36°	4891–4898	55–110	247 300

3. RESULTS

3.1. Cluster Reconstruction. A cluster can be defined as a set of adjacent samples with a signal amplitude higher than a certain threshold [4]. In order to take into account the signal fluctuations coming from the noise, it is required that for each anode at least two adjacent samples pass the threshold. Since the OLA amplifier has a linear response, for each channel the integral of the output signal is expected to be proportional to the charge collected by the anode. Under the condition that the threshold is sufficiently low compared to the maximum amplitude of the signal, that the signal has no undershoot, and that the sampling period is small enough compared to the signal shaping time, the sum of the sample linearized amplitudes of the cluster is, in a good approximation, proportional to the total collected charge. All these conditions were verified in our experiment. In the following, this sum will be called *charge*. The drift axis coordinate is calculated in first approximation as the time signal centroid multiplied by a uniform drift velocity, and the anode coordinate is calculated by the centroid of charge distribution measured on the anodes. After that, the systematic errors caused by the dopant inhomogeneities are successively corrected [7].

3.2. Cluster Size. A measurement of the cluster size was performed in the anode and the drift directions. The time evolution of the amplifier output signal results from the convolution of the anodic current and the time response of the amplifier. The anodic current shape is, in good approximation, similar to the electron collection time distribution. The nominal value of the OLA shaping time is 55 ns for a zero input capacity [11], but was larger and not known precisely in our experimental conditions. This uncertainly did not allow us to determine precisely the size of the electron cloud along the drift axis. However, since the shaping time of the OLA was constant during all the data taking and of the same order of magnitude of the anodic signal duration, a qualitative comparison of this duration is possible by calculating the drift direction cluster r.m.s. Figure 5 shows the distribution of the r.m.s. of the signal as

a function of the drift time for the various values of the incident angle. The Most Probable Values (MPV) of the signal r.m.s. as a function of the drift time are superimposed in Fig. 6. No significant difference is observed, confirming the independence of the cluster size along the drift axis versus the angle θ_{rz} .

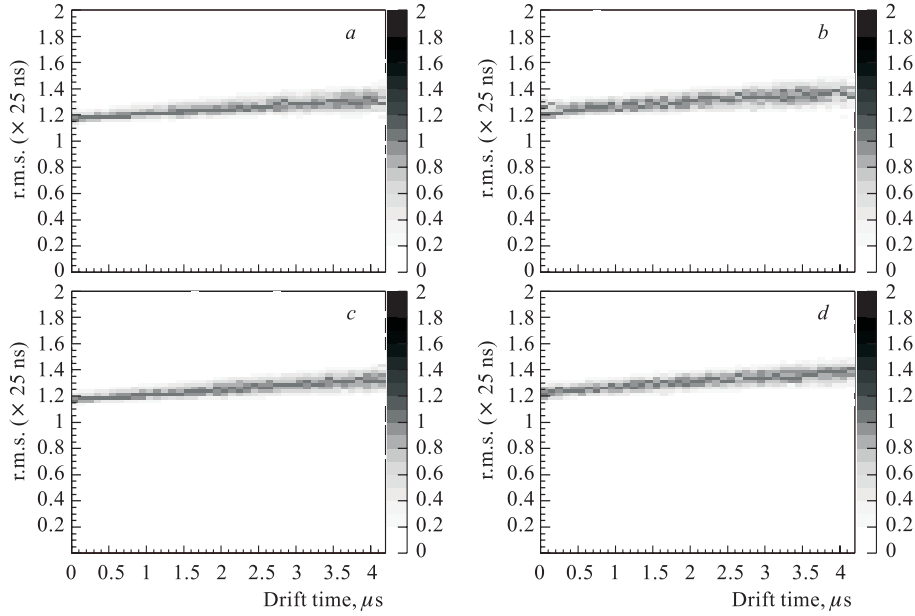


Fig. 5. Distributions of the drift direction cluster r.m.s. versus drift time; for different anode regions and beam incident angles: *a*) anodes 0–60, at 0° ; *b*) anodes 60–110, at 0° ; *c*) anodes 0–60, at 22° ; *d*) anodes 60–110, at 36°

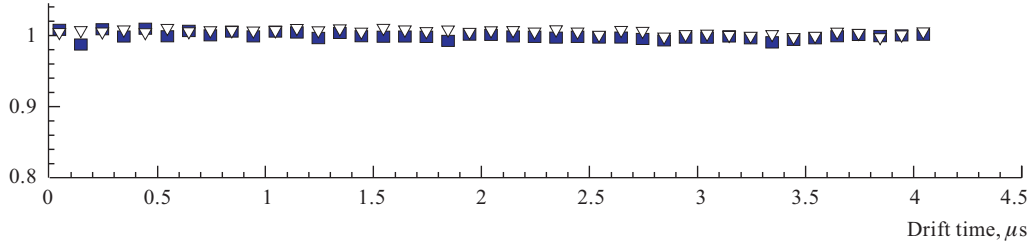


Fig. 6. Ratio of cluster sizes along the drift axis as a function of the drift time: ■ — $0^\circ/36^\circ$; ▽ — $0^\circ/22.5^\circ$

Figure 7 shows the relative amounts of clusters collected by one, two or three anodes as a function of the drift time for $\theta_{rz} = 0, 22.5, 36^\circ$. The number of clusters collected by more than three anodes is less than 1%. As expected, the number of multi-anode clusters increases with the inclination angle of the tracks. The number of single anode clusters in the anode region decreases with θ_{rz} changing from 11% of the total number of clusters for 0° to 4%

for 36° . The number of three anode clusters increases with drift time and θ_{rz} from 20% (for 0°) to 41% (for 36°) of the total amount of clusters.

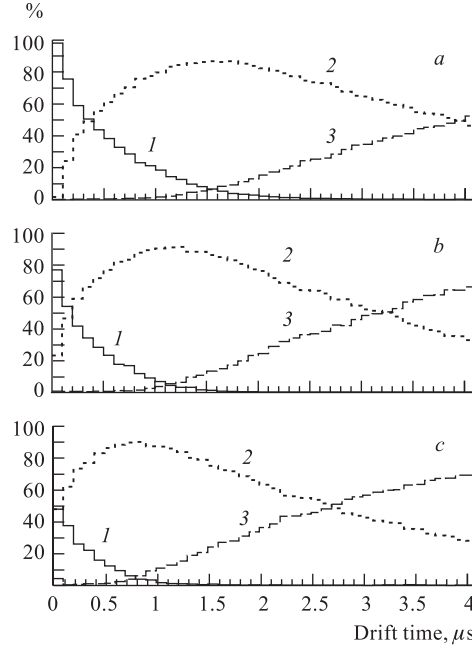


Fig. 7. Percentages of the events in which a cluster is collected by one (curve 1), two (curve 2) or three (curve 3) anodes as a function of the drift time: a) $\theta_{rz} = 0^\circ$; b) $\theta_{rz} = 22.5^\circ$; c) $\theta_{rz} = 36^\circ$

3.3. Charge. Figure 8, *a* shows the MPVs of the cluster charge versus the drift distance for the perpendicular tracks and inclined tracks for each group of the analyzed runs. Due to a defect of the used detector, the collected charge decreases as a function of the drift distance. Nevertheless, the ratio between the MPV for perpendicular tracks and the MPV for the inclined tracks has, apart from the experimental fluctuations, a constant value versus the drift time. The ratio between the MPVs for 0 and 22.5° (Fig. 8, *b*) is 0.917 ± 0.009 , which is in agreement with the expected value $\cos 22.5^\circ = 0.923$; the ratio between the MPVs for 0 and 36° gives 0.805 ± 0.011 , which is consistent with $\cos 36^\circ = 0.809$. This increase in the cluster size along the anode axis allows us to expect an improvement of the anodic resolution when θ_{rz} increases.

3.4. Anodic Resolution. The spatial resolution is defined as the r.m.s. of the residual distribution between the coordinate of the electron cloud measured by the SDD and the reference coordinate given by the microstrip telescopes. The coordinates measured by the SDD were corrected in order to take into account the systematic deviations caused by the dopant concentration inhomogeneities. The maps of the systematic deviations of the anodic coordinate were constructed from the beam test data. Figure 9 shows the maps for 0 and 22.5° . The circular structure can be attributed to the radial dependence of the dopant concentration fluctuations on the silicon wafer. Figure 10 shows the spatial resolution along the anode

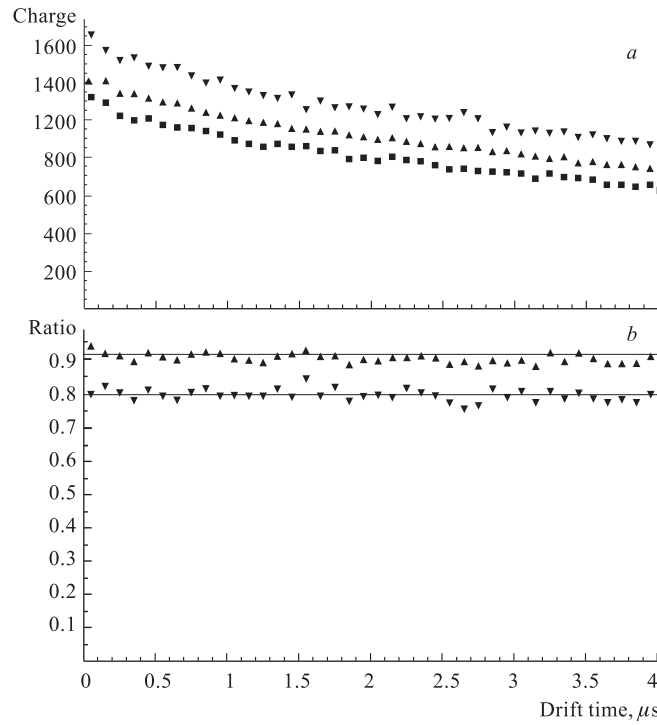


Fig. 8. *a*) Dependence of the most probable values of the charge collected for inclined tracks and for perpendicular tracks versus the drift time. *b*) Ratio of MPV of the charges versus drift time. The lines indicate the values of $\cos 22.5^\circ$ and $\cos 36^\circ$. ■ — at 0° ; ▲ — at 22° ; ▼ — at 36°

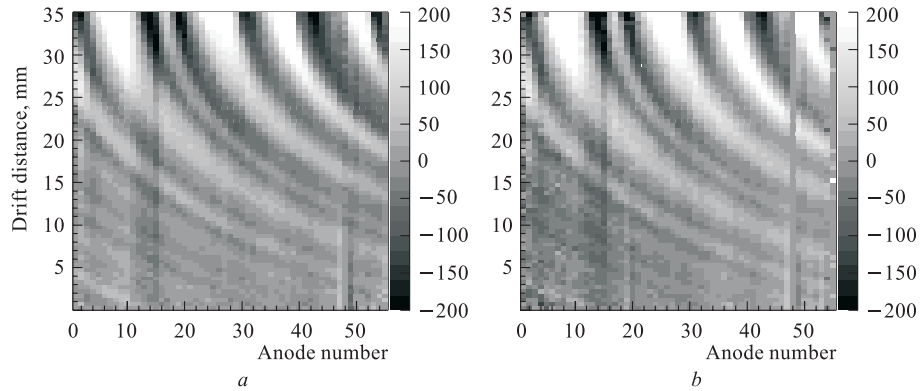


Fig. 9. Maps of systematic deviations of the SDD anodic coordinate of the electron cloud centroid with respect to the reference position of the crossing point of the particle for perpendicular (0° (*a*)) and inclined (22.5° (*b*)) tracks, as a function of the anode number and of the drift distance. The gray scale represents the amount of the deviation expressed in μm

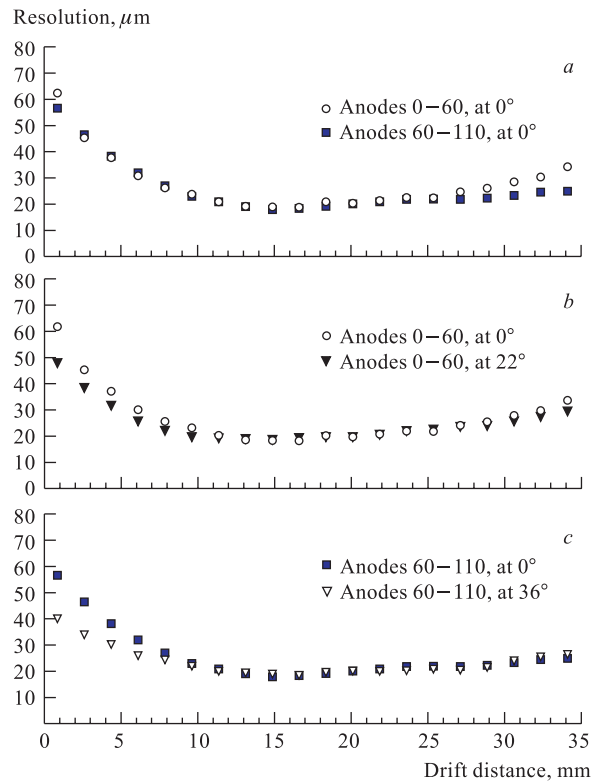


Fig. 10. Spatial resolution along the anode axis as a function of the drift distance: *a*) comparison of the resolution for the case of perpendicular tracks for two different regions of the SDD, corresponding to groups of the indicated anodes; *b*) comparison of the resolution for the case of tracks inclined at 22.5° and the perpendicular tracks obtained for the region between anodes 0 and 60; *c*) comparison of the resolution for the case of tracks inclined at 36° and perpendicular tracks for the group of anodes 60–110

direction as a function of the drift distance. The resolution for perpendicular tracks obtained for the two groups of anodes is presented in Fig. 10, *a*. At short drift distances, the anodic charge centroid is affected by uncertainty due to the charge cloud being much smaller than the anode pitch. As a consequence, the corresponding value of the resolution is higher than for longer drift distances. The deterioration of the resolution at the long drift distances is due to the decrease of the signal-to-noise ratio caused by the diffusion. The values of resolution for different groups of anodes are compatible for all drift distances, although there is an evident difference from distances larger than 25 mm. This discrepancy may come from the difficulty with correction for the large values of the systematic deviations (up to several hundreds of μm) in this region.

In Fig. 10, *b* the comparison between the measured resolution for perpendicular tracks and for an inclination of 22.5° in the SDD region between anodes 0 and 60 is shown. Figure 10, *c*

shows the comparison of the resolution for incident angles of 0 and 36°, obtained in the region corresponding to anodes 60–110. We observe that in the vicinity of the SDD anodes the values of the anodic resolution for inclined tracks become better with respect to those for perpendicular tracks. This behavior is caused by the decrease of the fraction of narrow clusters in the inclined track events. For longer drift distances the values of the resolution are very similar to those for perpendicular tracks. Except at short drift distances, the average value of the resolution is below 30 μm . The resolution reached the best value of 19 μm at a drift distance of 15 mm.

CONCLUSIONS

The results of the SDD data analysis for the inclined tracks, concerning total charge, are in excellent quantitative agreement with the expected behavior. The study of the cluster size and the spatial resolution is in agreement with expected results. In particular, the anode resolution at small drift paths is, on average, better for the inclined tracks than for the perpendicular tracks.

REFERENCES

1. *Gatti E., Rehak P.* // Nucl. Instr. Meth. A. 1984. V. 225. P. 608.
2. Technical Design Report of the Inner Tracking System. ALICE Collaboration. CERN/LHCC 99-12.
3. *Rashevsky A. et al.* // Nucl. Instr. Meth. A. 2001. V. 461. P. 133–138.
4. *Bonvicini W. et al.* // Ibid. V. 459. P. 494–501.
5. *Nouais D. et al.* // Nucl. Instr. Meth. A. 2002. V. 477. P. 99–103.
6. *Nouais D. et al.* // Nucl. Phys. B (Proc. Suppl.). 1999. V. 78. P. 252–258.
7. *Nouais D. et al.* // Nucl. Instr. Meth. A. 2001. V. 461. P. 222–225.
8. *Crescio E. et al.* CERN/ALICE/PUB 00-29. ALICE-INT-2001-09.
9. *Crescio E. et al.* Study of the Performance of the Silicon Drift Detectors of the ALICE Experiment. PhD thesis. www.to.infn.it/~crescio/tesipage.html
10. *Cerello P. et al.* ALICE-INT-2001-34.
11. *Dabrowski W. et al.* // Nucl. Phys. B. 1995. V. 44. P. 637.

Received on December 2, 2003.